CHEMISTRY OF MATERIALS
Cite This: Chem. Mater. 2018, 30, 2374−2378
Article
pubs.acs.org/cm

Facile Preparation of Light Emitting Organic Metal Halide Crystals with Near-Unity Quantum Efficiency

Chenkun Zhou,[†] Michael Worku,[‡] Jennifer Neu,[§] Haoran Lin,[†] Yu Tian,[‡] Sujin Lee,[†] Yan Zhou,[∥] Dan Han,[⊥,#,♦] Shiyou Chen,[⊥,#] Ayou Hao,[▽] Peter I. Djurovich,[○] Theo Siegrist,[†,§] Mao-Hua Du,[♦] and Biwu Ma*[,†,‡,∥]

[†]Department of Chemical and Biomedical Engineering, FAMU-FSU College of Engineering, Tallahassee, Florida 32310, United States
[‡]Materials Science and Engineering Program, Florida State University, Tallahassee, Florida 32306, United States
[§]National High Magnetic Field Laboratory, Florida State University, Tallahassee, Florida 32310, United States
[∥]Department of Chemistry and Biochemistry, Florida State University, Tallahassee, Florida 32306, United States
[⊥]Key Laboratory of Polar Materials and Devices, East China Normal University, Shanghai 200241, People's Republic of China
[#]Department of Physics, East China Normal University, Shanghai 200241, People's Republic of China
[▽]High-Performance Materials Institute (HPMI), Florida State University, Tallahassee, Florida 32306, United States
[○]Department of Chemistry, University of Southern California, Los Angeles, California 90089, United States
[♦]Materials Science & Technology Division, Oak Ridge National Laboratory, Oak Ridge, Tennessee 37831, United States

Supporting Information

ABSTRACT: We report the synthesis and characterization of $(Ph_4P)_2SbCl_5$, a novel ionically bonded organic metal halide hybrid with a zero-dimensional (0D) structure at the molecular level. By cocrystallization of tetraphenylphosphonium (Ph_4P^+) and antimony (Sb^{3+}) chloride salts, $(Ph_4P)_2SbCl_5$ bulk single crystals can be prepared in high yield, which exhibit a highly efficient broadband red emission peaked at 648 nm with a photoluminescence quantum efficiency (PLQE) of around 87%. Density functional theory (DFT) calculations reveal the origin of emission as phosphorescence from the excitons localized at $SbCl_5^{2-}$ with strong excited-state structural distortion. Interestingly, $(Ph_4P)_2SbCl_5$ bulk crystals with a PLQE of around 100% can be prepared via a rapid crystal growth process within minutes, followed by a spontaneous structural transformation. It was found that the rapid growth process yielded a yellow emitting kinetically favored metastable product containing solvent molecules, which turned into the red emitting thermodynamically stable product slowly at room temperature or quickly upon thermal treatment.

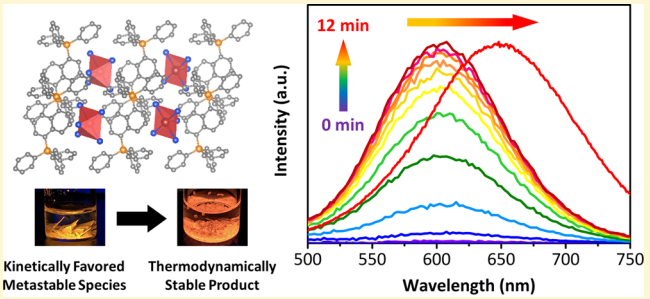

Light emitting materials have attracted tremendous research interest for their wide range of applications in display, lighting, bioimaging, etc.[1−5] As one of the most important classes of light emitting materials, phosphorescent metal complexes have achieved great successes in organic light emitting diodes with nearly 100% internal quantum efficiency.[6] However, most of the highly efficient phosphorescent complexes are based on either iridium or platinum, which are neither earth-abundant nor cost-effective. Also, their preparations often involve multiple steps of syntheses. Main group metal halides, e.g., germanium(II), tin(II), lead(II), antimony(III), and bismuth(III), have been previously reported to exhibit phosphorescence from metal-centered s−p transitions in fluid solution.[7−10] However, their room-temperature PLQEs are extremely low, which limits their potential applications in practical devices.

Recently, our group has developed several highly luminescent 0D organic metal halide hybrid crystals with near-unity PLQEs.[11,12] In these bulk crystals, distinct anionic metal halide species, such as $SnBr_6^{4-}$ and $SbCl_5^{2-}$, are completely isolated from each other and surrounded by large wide-bandgap organic cations. The site isolation eliminates electronic band formation between individual metal halide species, allowing bulk crystals to exhibit intrinsic properties of molecular metal halide species, with strongly Stokes shifted broadband emission due to significant excited state structural reorganization. These results prove that trapping luminescent metal halide species in an ionically bonded solid-state matrix to form an organic−

Received: January 10, 2018
Revised: March 9, 2018
Published: March 12, 2018

DOI: 10.1021/acs.chemmater.8b00129
Chem. Mater. 2018, 30, 2374−2378

inorganic hybrid material is an effective approach to preparing highly efficient light-emitting crystals. The key to realizing such 0D hybrid materials is to choose appropriate organic and inorganic salts that can cocrystallize to form crystalline structures.[12,13] The organic cations should have a large enough bandgap and size to ensure complete electronic site isolation of the photoactive inorganic species.

Here, we report the use of a tetraphenylphosphonium cation (Ph_4P^+) to assemble 0D organic antimony chloride $(Ph_4P)_2SbCl_5$ single crystals. Tetraphenylphosphonium salts were chosen for this investigation as they are well-known to readily form crystalline organic−inorganic hybrids.[14] Two facile synthetic routes have been established to prepare $(Ph_4P)_2SbCl_5$ single crystals in high yield, one by a slow solvent interdiffusion process and the other involving the rapid growth of a metastable product followed by spontaneous transformation to form the thermodynamically stable product. Photophysical properties of both metastable and stable $(Ph_4P)_2SbCl_5$ prepared by different methods were fully characterized. The metastable product, which is believed to contain solvent molecules, exhibits yellow emission peaked at 605 nm, and the stable product has red emission peaked at 648 nm with a near-unity PLQE.

Light yellow single crystals of $(Ph_4P)_2SbCl_5$ were prepared overnight in a 65% yield by diffusing the antisolvent diethyl ether into an undisturbed dimethylformamide (DMF) precursor solution of antimony trichloride ($SbCl_3$) and tetraphenylphosphonium chloride (Ph_4PCl) at room temperature in the N_2-filled glovebox. The ionic structure determined using single crystal X-ray diffraction (SCXRD; Tables S1, S2) adopts a triclinic space group $P\bar{1}$ where individual $SbCl_5^{2-}$ pyramids are surrounded by the large tetrahedral Ph_4P^+ cations (Figure 1a). A $SbCl_5^{2-}$ anion wrapped by several Ph_4P^+ cations

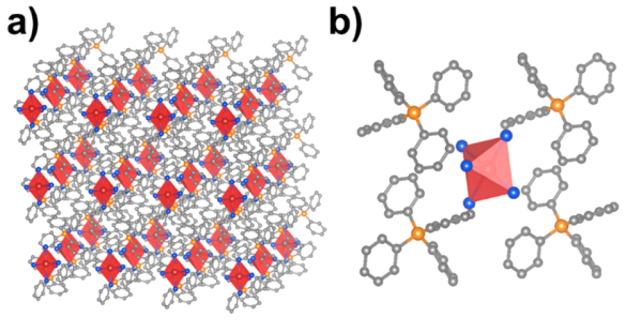

Figure 1. (a) View of the structure of $(Ph_4P)_2SbCl_5$ (red spheres, antimony atoms; blue spheres, chloride atoms; orange spheres, phosphorus atoms; gray spheres, carbon atoms; red polyhedra, $SbCl_5^{2-}$; hydrogen atoms are hidden for clarity). (b) View of an individual $SbCl_5^{2-}$ anion and nearest neighbor Ph_4P^+ cations.

is shown in Figure 1b. The bond distance between the Sb atom and the apical Cl atom in $SbCl_5^{2-}$ in $(Ph_4P)_2SbCl_5$ is 2.20 Å, which is noticeably shorter than distances of previously reported pyramidal $SbCl_5$ structures, such as $(Bmim)_2SbCl_5$ (2.37 Å)[15] and $(C_9NH_{20})_2SbCl_5$ (2.38 Å).[12] Meanwhile, the bond lengths beween the Sb atom and the other four Cl atoms are all between 2.61 and 2.63 Å, which are comparable to those in other $SbCl_5$ structures. The smaller pyramidal size suggests that the crystal structure of $(Ph_4P)_2SbCl_5$ is more compacted, which is not surprising considering the rigid phenyl groups facilitating molecular packing. The uniformity of the as-prepared crystals was confirmed by powder X-ray diffraction (PXRD; Figure S1). The consistency of PXRD patterns also suggests that there is no phase transition between 150 K and room temperature. The compositions of the crystals were further verified by elemental analysis. Details of synthesis and characterization can be found in the Supporting Information.

Bulk $(Ph_4P)_2SbCl_5$ crystals display bright red luminescence under UV irradiation (365 nm; Figure 2a). The photophysical properties of $(Ph_4P)_2SbCl_5$ samples were further characterized; details of experiments can be found in the Supporting Information. The excitation spectrum of $(Ph_4P)_2SbCl_5$ has a maximum at 375 nm (Figure 2b). The broadband red emission peaked at 648 nm has a full-width at half-maximum (FWHM) of 136 nm (Figure 2b) and a characteristic phosphorescent lifetime of 4.57 ± 0.09 μs (Figure 2c). Luminescence from $(Ph_4P)_2SbCl_5$ is significantly lower in energy than emission from $(C_9NH_{20})_2SbCl_5$ (λ_{max} = 590 nm)[10] and has a Stokes shift of 273 nm (1.41 eV). The large Stokes shift indicates $(Ph_4P)_2SbCl_5$ undergoes a larger structural distortion in the excited state than $(C_9NH_{20})_2SbCl_5$. The photoluminescent efficiency of the bulk crystals (PLQE = 87 ± 2%) is considerably high for red emitting materials (Figure S2). The $(Ph_4P)_2SbCl_5$ crystals also display high thermostability, as revealed by thermogravimetric analysis, with no degradation until 300 °C (Figure S3) and excellent photostability under continuous high-power mercury lamp irradiation (150 mW/cm^2; Figure S4).

Density functional theory (DFT) calculations were performed to shed light on the photophysical properties of $(Ph_4P)_2SbCl_5$. The calculated electronic structure of $(Ph_4P)_2SbCl_5$ shows a $SbCl_5$-derived valence band and a Ph_4P-derived conduction band (Figure S5). The strong hybridization between the occupied Sb-5s oritital and the Cl-3p orbital that points to the Sb ion creates an antibonding orbital of Sb-5s and Cl-3p, which is higher in energy than the other Cl-3p orbitals. This results in the top valence band that is split off from the rest of the valence band, as seen in Figure S5. This band is nearly dispersionless due to the long Sb−Sb distance. The conduction band is mainly made up of the antibonding π states on Ph_4P molecular cations. The empty Sb-5p band is located within the Ph_4P-dominated conduction band as shown in Figure S5b. Although the Sb-5p level is above the conduction band minimum at the ground state, we find that the excited electron prefers to be localized at $SbCl_5$ due to the strong Coulomb binding between the electron and the hole. We tested two types of excitons, one localized at $SbCl_5$ (EX1) and the other of the charge transfer type (EX2) with the hole localized at the $SbCl_5$ cluster and the electron at the adjacent Ph_4P molecule. Table S3 compares the energies of the spin-triplet and spin-singlet EX1 and EX2. The most stable exciton is the spin-triplet EX1 localized at $SbCl_5$; the partial charge density contours of the electron and the hole wave functions of this exciton are plotted in Figure 3. The calculated emission energy of the spin-triplet EX1 is 1.91 eV, matching perfectly with the experimentally measured emission peak at 1.91 eV (648 nm). The spin-triplet exciton emission is also consistent with the observed lifetime of the emission on the order of microseconds. The calculated excitation energy is 3.68 eV, within the experimentally measured excitation band, and the calculated Stokes shift is 1.77 eV. Such a large Stokes shift is largely due to structural reorganization in the excited state, which lowers the exciton energy by 0.96 eV. The exciton relaxation involves the shortening of the four Sb−Cl bonds on the $SbCl_4$ plane and the elongation of the Sb−Cl bond

DOI: 10.1021/acs.chemmater.8b00129
Chem. Mater. 2018, 30, 2374−2378

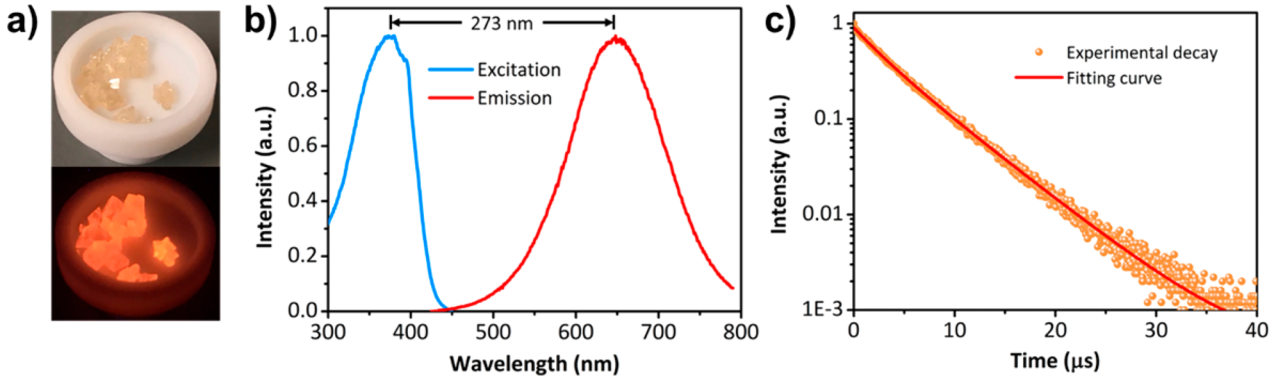

Figure 2. (a) Images of bulk crystals produced via antisolvent vapor diffusion method under ambient light (top) and UV light (365 nm, bottom). (b) Excitation and emission spectra of bulk $(Ph_4P)_2SbCl_5$ crystals. (c) Luminescence decay profile of bulk $(Ph_4P)_2SbCl_5$ crystals.

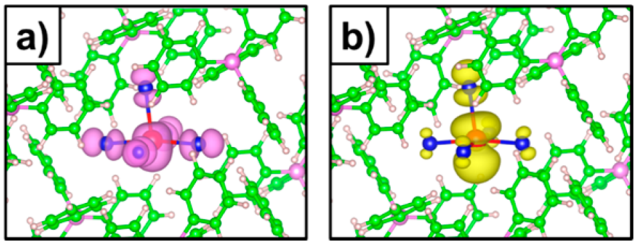

Figure 3. Partial charge density contours of (a) the hole and (b) the electron wave functions of the most stable exciton in $(Ph_4P)_2SbCl_5$.

perpendicular to the four shortened bonds. The significant elongation of the vertical Sb−Cl bond during the exciton relaxation may hold the key to the understanding of the different Stokes shifts observed in $(Ph_4P)_2SbCl_5$ and $(C_9NH_{20})_2SbCl_5$, which have different vertical Sb−Cl bond lengths of 2.20 and 2.38 Å, respectively, at the ground state. As the Stokes shift is caused by the excited state structural distortion, the larger Stokes shift for $(Ph_4P)_2SbCl_5$ than $(C_9NH_{20})_2SbCl_5$ is likely due to a stronger excited state distortion from a shorter Sb−Cl bond.

The extremely high PLQEs of $(Ph_4P)_2SbCl_5$ and many other 0D organic metal halide hybrids make them highly promising emitters for a variety of applications. However, the relatively slow crystal growth process for their preparation presents a drawback. It is therefore of great interest to develop quicker processes to grow bulk metal halide hybrid crystals. Considering the ease of crystallization for the PPh_4^+ salts, we attempted to prepare $(Ph_4P)_2SbCl_5$ in an accelerated crystal growth process. By directly injecting a fixed amount of diethyl ether into the DMF precursor solution at room temperature, plate-like crystals quickly grew out of the solution within minutes as shown in the video (see Supporting Information). Increasing the amount of diethyl ether resulted in faster crystallization of plate-like crystals with reduced crystal size.

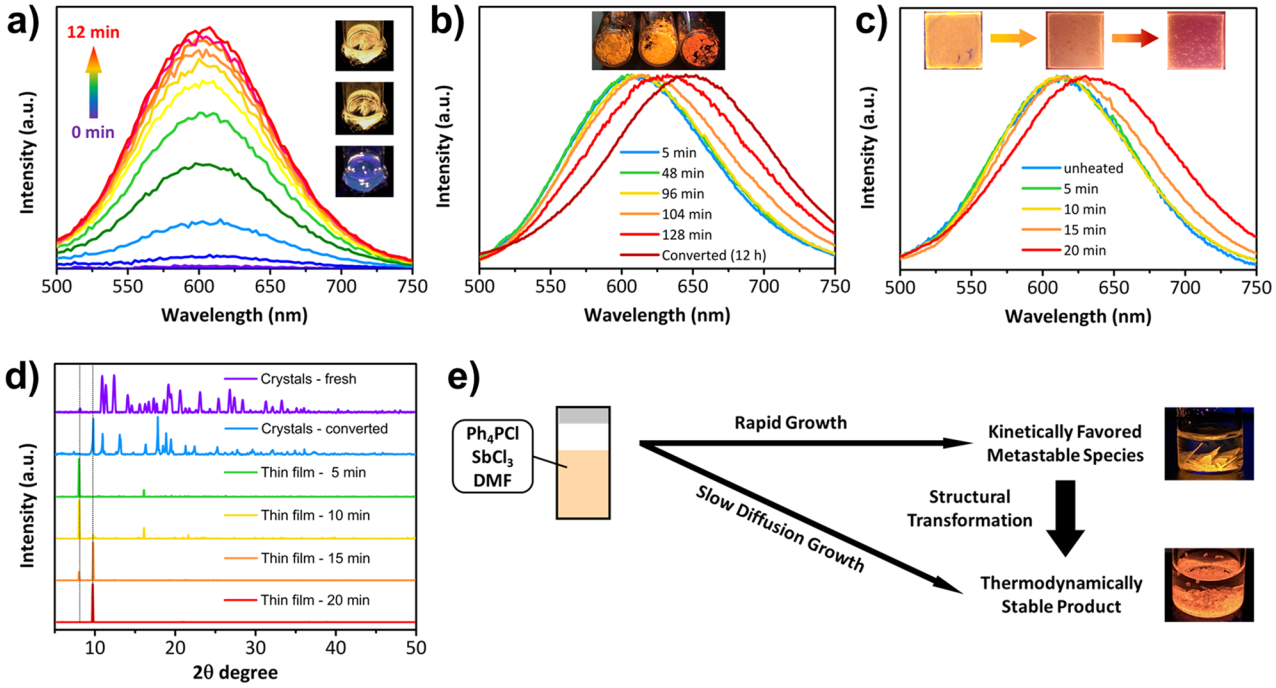

Figure 4. (a) *In situ* photoluminescence spectra of bulk crystals during rapid crystal growth. (b) Photoluminescence spectra change of bulk crystals after removal of the precursor solution. (c) Photoluminescence spectra of thin films upon different heat treatment times. (d) PXRD patterns of metastable crystals and thin films upon different heat treatment times. (e) Schematic description of crystal growth pathways of $(Ph_4P)_2SbCl_5$.

DOI: 10.1021/acs.chemmater.8b00129
Chem. Mater. 2018, 30, 2374−2378

Interestingly, the crystals produced by this rapid growth method exhibited yellow emission peaking at around 600 nm upon UV excitation (365 nm). The intensity of broadband emission increases without a change of spectral line shape during the crystal growth process, as revealed by the *in situ* photoluminescence measurements (Figure 4a). After these yellow emitting crystals were collected and stored in the N_2-filled glovebox, their emission was found to gradually shift from yellow (λ_{max} = 600 nm) to red (λ_{max} = 648 nm; Figure 4b). It should be pointed out that the optical properties of fully converted crystals from rapid growth are almost identical to the crystals prepared by the slow vapor diffusion method. An even higher PLQE of 99 ± 1% was achieved for converted crystals from rapid growth, which is possibly due to fewer defects in these crystals.

The distinct optical properties of crystals prepared by slow and rapid processes suggested that a metastable phase was likely a kinetically favored product formed during the latter growth process, which subsequently undergoes structural transformation to the thermodynamically stable phase. To support our hypothesis, we have prepared a $(Ph_4P)_2SbCl_5$ thin film by spin-casting a DMF precursor solution, followed by heat treatment in a N_2-filled glovebox. As shown in Figure 4c, the as-cast thin film exhibits yellow emission, exactly the same as that of rapid grown crystals in solution, which becomes red emitting upon thermal treatment, suggesting the transformation from a kinetically favored product into a thermodynamically stable product. The structural difference between the two phases was characterized using PXRD and is shown in Figure 4d. The PXRD patterns of thin films show that the peak at 8° vanished while a peak at 9.8° increased over time, confirming the formation of the thermodynamically stable product. Therefore, the crystal growth mechanisms can be depicted in Figure 4e; i.e., rapid growth forms a kinetically favored metastable product, and the slow diffusion process results in a thermodynamically stable product. As solvent effects on the electronic spectra of molecules in solution have been well established,[16] it is reasonable to suspect that the variation of emission can be attributed to the removal of solvent molecules in crystals and thin films. In the rapid crystal growth process, polar solvent molecules (i.e., DMF) can cocrystallize with Ph_4P^+ and $SbCl_5^{2-}$ to form a metastable structure, as confirmed by ^1H NMR spectra (Figure S6), which turns into a thermodynamically stable phase without solvent molecules. Upon heat treatment, this structural transformation process can be expedited. TGA measurements of the fresh and converted metastable crystals (Figure S3) clearly show a sizable weight loss for the metastable crystal at around 100 °C, corresponding to the removal of DMF molecues. In contrast, there is little-to-no weight loss for the converted crystal and the crystal prepared by a slow diffusion method, remaining stable up to 300 °C.

In summary, we have established facile synthetic approaches for the preparation of single crystalline organic antimony chloride hybrid $(Ph_4P)_2SbCl_5$, which exhibits strongly Stokes shifted red emission with a near-unity quantum efficiency, as a result of the localized molecular transition in $SbCl_5$ with pronounced excited state structural distortion. Besides a conventional slow solvent vapor diffusion process, a rapid crystal growth approach was developed to prepare these light-emitting crystals in high yield, by taking advantage of the easy crystallization of tetraphenylphosphonium salts. Both kinetically favored metastable and thermodynamically stable crystals have been identified and characterized. Our discovery of facile preparation of low cost, ecofriendly, high performance light emitting crystals represents a major breakthrough in the field of light emitting materials, which is both scientifically and practically meaningful.

■ ASSOCIATED CONTENT

Supporting Information

The Supporting Information is available free of charge on the ACS Publications website at DOI: 10.1021/acs.chemmater.8b00129.

Syntheses and characterizations of the organic antimony chloride crystals and results (PDF)
Crystallographic information (CIF)
A video showing the rapid crystal growth (MPG)

■ AUTHOR INFORMATION

Corresponding Author

*E-mail: bma@fsu.edu.

ORCID

Shiyou Chen: 0000-0002-4039-8549
Mao-Hua Du: 0000-0001-8796-167X
Biwu Ma: 0000-0003-1573-8019

Notes

The authors declare no competing financial interest.

■ ACKNOWLEDGMENTS

The authors acknowledge the support from the National Science Foundation (DMR-1709116 and CHE-1664661). The work at the Oak Ridge National Laboratory was supported by the Department of Energy, Office of Science, Basic Energy Sciences, Materials Sciences and Engineering Division. D.H. and S.C. were supported by the State Scholarship Fund in China and CC of ECNU. The authors thank Dr. Kenneth Hanson at the Florida State University for the access to a spectrophotometer and Dr. Hanwei Gao for the access to the instrument for the photostability test.

■ REFERENCES

(1) Baldo, M.; Lamansky, S.; Burrows, P.; Thompson, M.; Forrest, S. Very High-Efficiency Green Organic Light-Emitting Devices Based on Electrophosphorescence. *Appl. Phys. Lett.* **1999**, *75*, 4−6.

(2) Cui, Y.; Chen, B.; Qian, G. Lanthanide Metal-Organic Frameworks for Luminescent Sensing and Light-Emitting Applications. *Coord. Chem. Rev.* **2014**, *273*−*274*, 76−86.

(3) Vinck, E. M.; Cagnie, B. J.; Cornelissen, M. J.; Declercq, H. A.; Cambier, D. C. Increased Fibroblast Proliferation Induced by Light Emitting Diode and Low Power Laser Irradiation. *Lasers in med. sci.* **2003**, *18*, 95−99.

(4) Thirumal, K.; Chong, W. K.; Xie, W.; Ganguly, R.; Muduli, S. K.; Sherburne, M.; Asta, M.; Mhaisalkar, S.; Sum, T. C.; Soo, H. S.; Mathews, N. Morphology-Independent Stable White-Light Emission from Self-Assembled Two-Dimensional Perovskites Driven by Strong Exciton−Phonon Coupling to the Organic Framework. *Chem. Mater.* **2017**, *29*, 3947−3953.

(5) Dohner, E. R.; Jaffe, A.; Bradshaw, L. R.; Karunadasa, H. I. Intrinsic White-Light Emission from Layered Hybrid Perovskites. *J. Am. Chem. Soc.* **2014**, *136*, 13154−13157.

(6) Baldo, M.; Thompson, M.; Forrest, S. High-Efficiency Fluorescent Organic Light-Emitting Devices Using a Phosphorescent Sensitizer. *Nature* **2000**, *403*, 750−753.

(7) Nikol, H.; Vogler, A. Photoluminescence of Antimony (III) and Bismuth (III) Chloride Complexes in Solution. *J. Am. Chem. Soc.* **1991**, *113*, 8988−8990.

DOI: 10.1021/acs.chemmater.8b00129
Chem. Mater. 2018, 30, 2374−2378

(8) Nikol, H.; Becht, A.; Vogler, A. Photoluminescence of Germanium (II), Tin (II), and Lead (II) Chloride Complexes in Solution. *Inorg. Chem.* **1992**, *31*, 3277−3279.
(9) Oldenburg, K.; Vogler, A. Electronic Spectra and Photochemistry of Tin (II), Lead (II), Antimony (III), and Bismuth (III) Bromide Complexes in Solution. *Z. Naturforsch. B Chem. Sci.* **1993**, *48*, 1519−1523.
(10) Evans, R. C.; Douglas, P.; Winscom, C. J. Coordination Complexes Exhibiting Room-Temperature Phosphorescence: Evaluation of Their Suitability as Triplet Emitters in Organic Light Emitting Diodes. *Coord. Chem. Rev.* **2006**, *250*, 2093−2126.
(11) Zhou, C.; Tian, Y.; Wang, M.; Rose, A.; Besara, T.; Doyle, N. K.; Yuan, Z.; Wang, J. C.; Clark, R.; Hu, Y.; Siegrist, T.; Lin, S.; Ma, B. Low-Dimensional Organic Tin Bromide Perovskites and Their Photoinduced Structural Transformation. *Angew. Chem. Int. Ed.* **2017**, *56*, 9018−9022.
(12) Zhou, C.; Lin, H.; Tian, Y.; Yuan, Z.; Clark, R.; Chen, B.; van de Burgt, L. J.; Wang, J. C.; Zhou, Y.; Hanson, K.; Meisner, Q. J.; Neu, J.; Besara, T.; Siegrist, T.; Lambers, E.; Djurovich, P.; Ma, B. Luminescent Zero-Dimensional Organic Metal Halide Hybrids with Near-Unity Quantum Efficiency. *Chem. Sci.* **2018**, *9*, 586−593.
(13) Zhou, C.; Lin, H.; Shi, H.; Tian, Y.; Pak, C.; Shatruk, M.; Zhou, Y.; Djurovich, P.; Du, M.; Ma, B. A Zero-Dimensional Organic Seesaw-Shaped Tin Bromide with Highly Efficient Strongly Stokes-Shifted Deep-Red Emission. *Angew. Chem. Int. Ed.* **2018**, *57*, 1021−1024.
(14) Xu, L.-J.; Sun, C.-Z.; Xiao, H.; Wu, Y.; Chen, Z.-N. Green-Light-Emitting Diodes based on Tetrabromide Manganese(II) Complex through Solution Process. *Adv. Mater.* **2017**, *29*, 1605739.
(15) Wang, Z.-P.; Wang, J.-Y.; Li, J.-R.; Feng, M.-L.; Zou, G.-D.; Huang, X.-Y. $[Bmim]_2SbCl_5$: A Main Group Metal-Containing Ionic Liquid Exhibiting Tunable Photoluminescence and White-Light Emission. *Chem. Commun.* **2015**, *51*, 3094−3097.
(16) McRae, E. Theory of Solvent Effects on Molecular Electronic Spectra. Frequency Shifts. *J. Phys. Chem.* **1957**, *61*, 562−572.

DOI: 10.1021/acs.chemmater.8b00129
Chem. Mater. 2018, 30, 2374−2378